

We are IntechOpen, the world's leading publisher of Open Access books Built by scientists, for scientists

4,800

Open access books available

122,000

International authors and editors

135M

Downloads

Our authors are among the

154

Countries delivered to

TOP 1%

most cited scientists

12.2%

Contributors from top 500 universities

**WEB OF SCIENCE™**Selection of our books indexed in the Book Citation Index
in Web of Science™ Core Collection (BKCI)

Interested in publishing with us?
Contact book.department@intechopen.com

Numbers displayed above are based on latest data collected.

For more information visit www.intechopen.com

Mechanisms of Defibrillation Failure

Takashi Ashihara¹, Jason Constantino² and Natalia A. Trayanova²

¹*Shiga University of Medical Science,*

²*Johns Hopkins University,*

¹*Japan*

²*U.S.A.*

1. Introduction

Since defibrillation by high-energy electric shocks is the only effective means for termination of ventricular fibrillation, defibrillation shocks are now widely used in clinical practice for prevention of sudden cardiac death. However, the high-energy shocks could result in myocardial dysfunction and damage (Runsio et al., 1997) and in psychological trauma (Maisel, 2006). Comprehensive understanding of the ventricular response to electric shocks as well as the mechanisms of defibrillation failure is the approach most likely to succeed in reducing shock energy.

Recent experimental techniques, such as high-resolution mapping with multi-electrodes or optical recordings, have provided new characterizations of tissue responses to electric shocks. However, the mechanisms of the success and failure of defibrillation are not fully understood since the presently available experimental techniques, which provide detailed information about the myocardial surface (mostly epicardial) activity, are insufficient in resolving depth information during and after the electric shocks. Moreover, electrical or optical signal artifacts during the shock make it difficult for the researchers to get direct evidence regarding the mechanisms of electrical defibrillation.

It has been demonstrated experimentally that after the delivery of shocks of strength near the defibrillation threshold (DFT) from an implantable cardioverter-defibrillator (ICD) device, the first global activation consistently arises focally on the left ventricle (LV) (Chattipakorn et al., 2001, 2003) following an isoelectric window (a quiescent period following the shock). Understanding the origins of the isoelectric window is thus of great importance for uncovering the mechanisms of defibrillation failure. Various hypothesis have been proposed for the existence of the isoelectric window, including virtual electrode-induced propagated graded response (Trayanova et al., 2003), calcium sinkholes (Hwang et al., 2006), and activations emanating from Purkinje fibers (Dodd et al., 2007); however, the mechanisms responsible for it remain inconclusive.

In this context, we hypothesized that submerged “tunnel propagation” of postshock activation (PA) through shock-induced intramural excitable areas underlies both fibrillation induction and failed defibrillation by shocks as well as the existence of an isoelectric window. To test this hypothesis, we analyzed the global three-dimensional activity in ventricles with the use of a recently-developed realistic computer model of stimulation/defibrillation in the rabbit heart (Trayanova et al., 2002). Simulations with this

model, termed the rabbit bidomain model of defibrillation, have proven invaluable in understanding various aspects of the response of the heart to shocks (Rodriguez et al., 2005). The bidomain model is a continuum representation of the myocardium, which takes into account both intracellular and extracellular current distributions through the myocardium. The objectives of this book chapter are to demonstrate the use of the realistic three-dimensional bidomain rabbit ventricular model and failed defibrillation in uncovering the mechanisms of fibrillation induction and defibrillation failure.

2. Similarities between fibrillation induction and failed defibrillation

An isoelectric window (Chen et al., 1986a), the quiescent period prior to the first global PA, has been experimentally documented following strong shocks. The presence of the isoelectric window following failed defibrillation attempts (Chen et al., 1986a; Shibata et al., 1988b; Wang et al., 2001) led to the understanding that an electric shock terminates ongoing fibrillation but then reinitiates it. Hence, the mechanisms of fibrillation induction and its reinitiation (failed defibrillation) are considered to be the same. Thus, elucidating the origin of PAs resulting in fibrillation induction provides invaluable insight into the mechanisms of defibrillation failure and could contribute significantly in finding novel ways to appreciably lower the shock energy.

Indeed, striking similarities between these mechanisms have been found, particularly with regard to the propagation of the first global PA and the duration of the isoelectric window (Shibata et al., 1988a, 1988b; Wang et al., 2001). The similarity is supported by the significant correlation between the upper limit of vulnerability (ULV) and DFT (Chen et al., 1986b; Swerdlow et al., 1998). Based on these facts, we first focused on the mechanism responsible for the earliest-propagating PA in fibrillation induction by the electric shock, and then we extend the study to defibrillation failure.

3. Fibrillation induction following external shock

First, we conducted simulations of fibrillation induction following uniform-field external shocks with the use of the rabbit bidomain ventricular model, extensively validated with experimental measurements (Rodriguez et al., 2005). Biphasic shocks were delivered via plate electrodes located in the vicinity of RV and LV free walls (Figure 1A). The ventricles were immersed in the perfusing bath.

Figure 1B shows examples of arrhythmia non-induction and induction after 16- and 12-V/cm shocks, which are just above and near the ULV, respectively. Virtual electrodes (regions of positive and negative membrane polarization) induced by the shock (shock end, 0-ms panels) resulted in quick excitation of the ventricular surface (10-ms panels). Whereas no PA was induced by the 16-V/cm shock, for the 12-V/cm shock case, the earliest-propagated PA (arrows in 55-ms panel) led to the establishment of ventricular fibrillation (VF) (80-ms panel) following an isoelectric window.

The origin of the initiating PA following the 12-V/cm shock is analyzed in Figure 1C. The initiating PA originated at the boundary between a recovered area unaffected by the shock and the shock-induced depolarized area as a virtual electrode-induced propagated graded response (zigzag arrow in 10-ms panel). This occurred deep within the LV wall, and the initiating PA proceeded transmurally toward the LV epicardium (20-ms panel), where tissue had already recovered, and became the earliest-propagated PA.

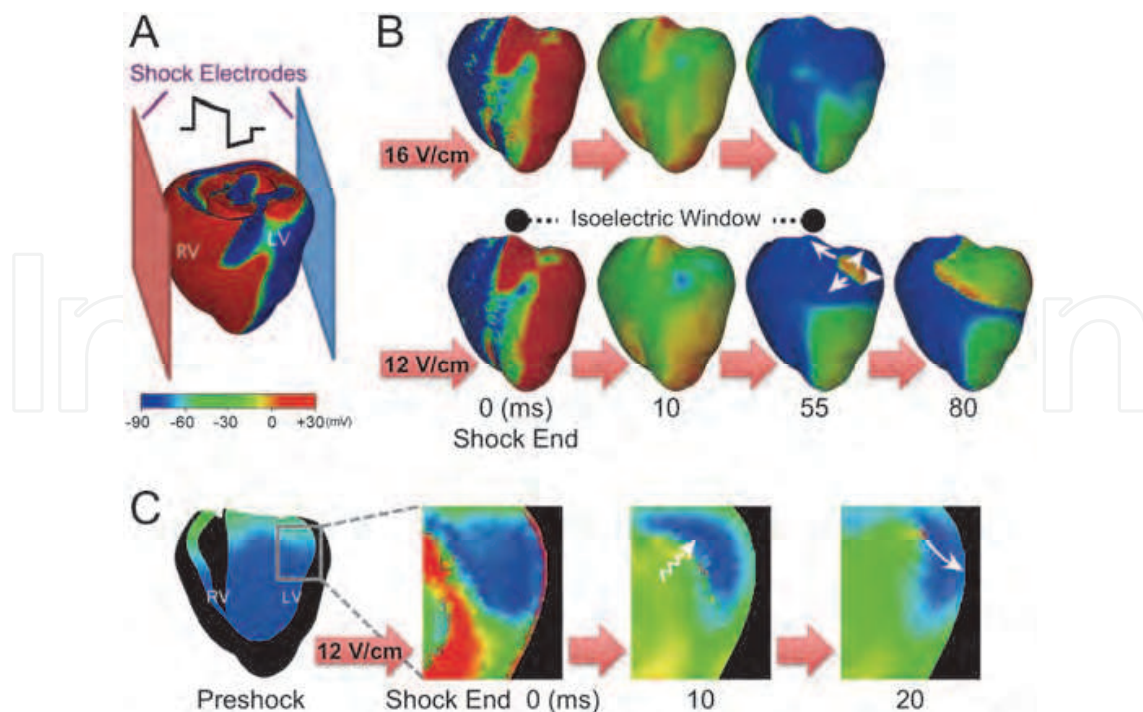


Fig. 1. Fibrillation induction following external biphasic shock.

4. Defibrillation failure following an ICD shock

We then extended the simulation study to electrical defibrillation by nonuniform-field ICD shocks. Biphasic shocks were delivered via ICD electrodes, a catheter in RV and an active can in the bath near the posterior LV (Figure 2A). For near-DFT shock episodes, we examined PA origins, and we found that around half of the earliest-propagated PAs originated from shock-induced wavefronts and the other half from pre-existing wavefronts. This means that failed defibrillation for near-DFT shocks is not always associated with termination of pre-existing wavefronts and generation of new wavefronts by the shock.

As shown in Figure 2B, the postshock excitable area in the RV after near-DFT shocks was directly depolarized by the shock and the one in the septum was immediately eradicated by break excitations elicited by the shock (black circles in 0- and 17-ms panels), whereas the main postshock excitable area was consistently located within the LV wall (red ellipsoid in 17-ms panel) since ICD electrodes generate weak virtual electrode polarization across the thick LV wall. Thus, the majority of postshock LV excitable area resulted from pre-existing excitable gaps during VF at the time of shock. This means that the larger excitable area in the LV wall allowed for postshock wavefronts of different origins to propagate unobstructed, increasing the likelihood of defibrillation failure. Thus, defibrillation shock outcome was affected by the preshock state.

As shown in Figure 2C, whereas the earliest-propagated PA arose on the epicardium immediately after the 75-V shock end (white arrows in top panel), the increase in shock strength to 100 V changed the type of the earliest-propagated PA into a delayed breakthrough after an isoelectric window (middle panel). Further increase in the shock strength to 175 V caused the prolongation of the isoelectric window from 35 to 50 ms (compare middle and bottom panels). These simulation results suggest that high strength shocks caused the entire epicardium to become refractory and created midmyocardial

excitable tunnel, through which a submerged initiating PA propagated during the isoelectric window, i.e., tunnel propagation occurred. After the isoelectric window, the initiating PA became the earliest-propagated PA, often reinitiating VF.

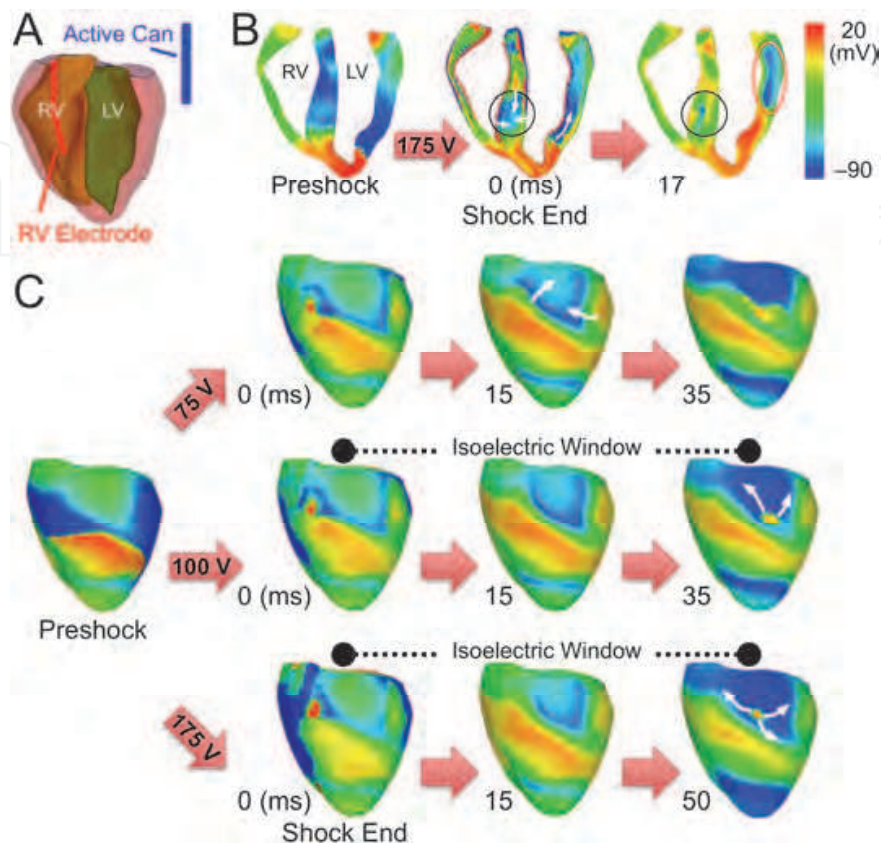


Fig. 2. Failed defibrillation following ICD shock.

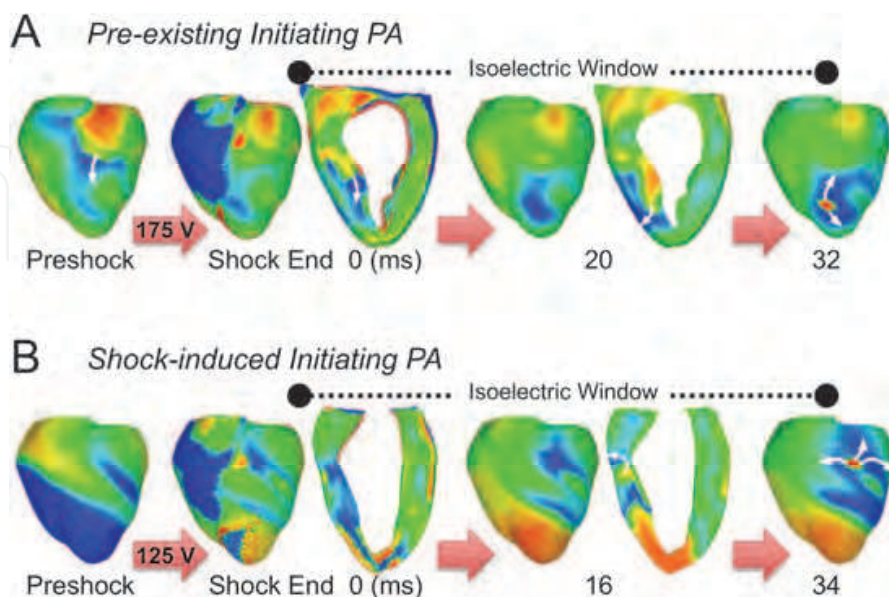


Fig. 3. Examples of initiating PA following ICD shock.

We classified the events depending on the origin of the initiating PA, which was either pre-existing fibrillatory or shock-induced wavefront.

Figure 3A shows an example of the tunnel propagation of pre-existing initiating PA after the near-DFT shock. A pre-existing fibrillatory epicardial wavefront (arrow in preshock panel) became submerged at shock end (arrow in 0-ms panel) and propagated within the midmyocardial tunnel following the 175-V shock (arrow in 20-ms panel). The tunnel formation and the submerging of the wavefront were due to the epicardium becoming refractory after this near-DFT shock (compare epicardial regions in 0- and 20-ms panels), resulting in an isoelectric window of LV epicardium. Tunnel propagation ended in a breakthrough (exit from the tunnel) on the near LV apex after the isoelectric window (32-ms panel), causing the shock to fail.

In contrast, Figure 3B shows an example of the tunnel propagation of initiating PA induced by near-DFT shock. There was no pre-existing wavefront, resulting in initiating PA at shock end (0-ms panel). After the 125-V shock, a new shock-induced wavefront propagated intramurally through the LV tunnel (arrow in 16-ms panel), emerging focally on the LV epicardium after the isoelectric window (34-ms panel), and causing the shock to fail.

5. Implications of the tunnel propagation hypothesis

The external monophasic shock study from our group (Rodriguez et al., 2005) demonstrated that shock outcome and the type of postshock arrhythmia depend on the distribution of the intramural excitable area (tunnel) formed by shock-induced deexcitation of previously refractory myocardium. We extended these findings and proposed the “tunnel propagation” hypothesis (Ashihara et al., 2008) for shock-induced arrhythmogenesis that unifies all known aspects and findings regarding the postshock electric behavior of the heart, e.g., mechanisms of PA origin and isoelectric window after electric shocks, and the increase in isoelectric window duration for high strength shocks. Furthermore, we found that the tunnel propagation hypothesis is applicable to not only arrhythmia induction with external uniform-field shocks (Ashihara et al., 2008) but also defibrillation failure following nonuniform-field ICD shocks (Constantino et al., 2010).

As previously suggested by the ULV hypothesis (Chen et al., 1986a; Shibata et al., 1988b; Wang et al., 2001), failed defibrillation by near-DFT shock may result from the reinitiation of VF following the isoelectric window since the pre-existing VF is entirely terminated by the shock (Figure 4A). If this is the case, the shock outcome must not be affected by the preshock state of ventricles. However, both defibrillation shock outcome and the DFT have probabilistic nature (Davy et al., 1987; Yashima et al., 2003). The tunnel propagation hypothesis (Figure 4B) explains surmises that for successful defibrillation, pre-existing wavefronts may not be terminated by the strong shock but instead remain hidden in the intramural tunnel, in contrast to what was previously believed. Moreover, the tunnel propagation hypothesis can link defibrillation shock outcome to the preshock state of the ventricles. Based on the tunnel propagation hypothesis, both pre-existing and new shock-induced wavefronts propagate through the intramural excitable tunnel during the isoelectric window before the reinitiation of VF (defibrillation failure), and therefore the probability of defibrillation failure varies depending on the timing of shock delivery during VF. In fact, here we observed in the simulations that postshock propagation within the LV mid-myocardium was strongly dependent on preshock state.

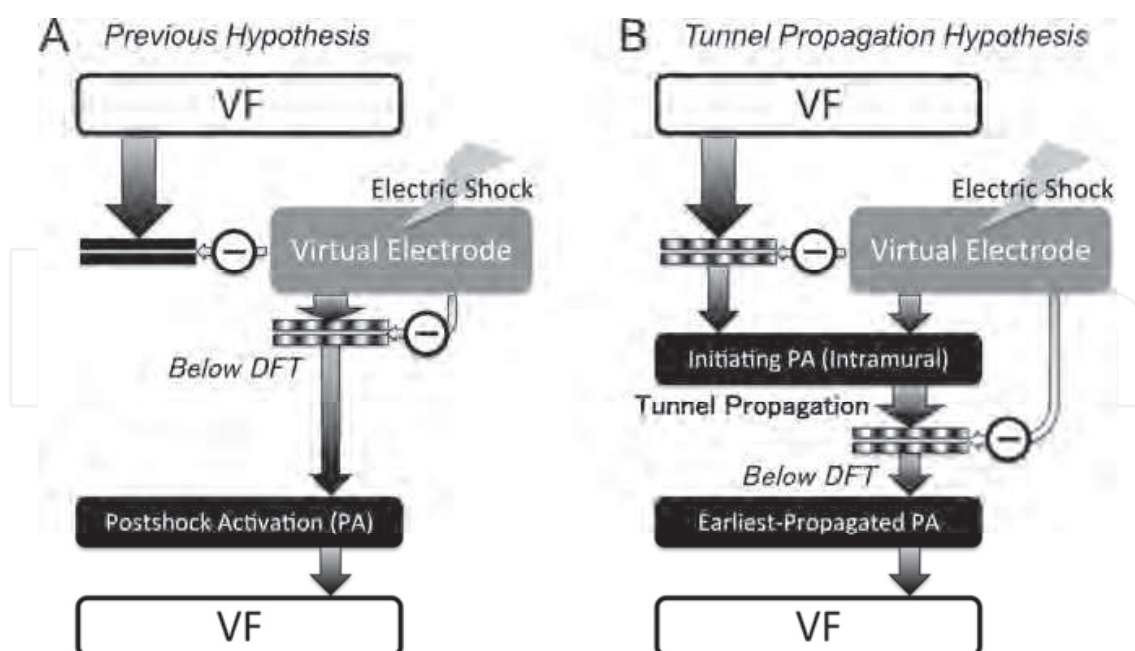


Fig. 4. Comparison between the previous hypothesis for VF reinitiation and the tunnel propagation hypothesis.

However, the concepts proposed here do not limit the origin of the initiating PAs; these might have alternative origins, such as Purkinje fibers (Dodd et al., 2007). The tunnel hypothesis is independent of the origin of wavefronts that propagate through it.

The increase in isoelectric window after high strength shock can also be explained by the prolongation of the epicardial refractoriness (surface polarization), resulting in the longer tunnel propagation. This is because intramural virtual electrode polarization is lower magnitude than surface polarization (Entcheva et al., 1999) and thus the LV mid-myocardium, less affected by the shock, still contributes to the excitable tunnel even for higher strength shocks.

Considering the high probability of the existence of the postshock excitable tunnel even for above-DFT shocks, defibrillation success may be explained by the fact that initiating PAs, originating within the wall, cannot find an excitable exit onto the epicardium and die out in the mid-myocardium. Obtaining such insight into the mechanisms of defibrillation would have been impossible with the use of experimentation alone.

6. Conclusion

The tunnel propagation hypothesis, as part of the set of mechanisms operating during defibrillation, is expected to shed light on possible strategies for lowering DFT as well as for developing new defibrillation devices.

7. Funding sources

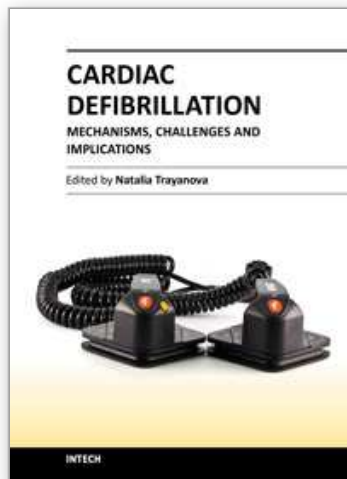
This work was supported by Grant-in-Aid 21790717, 22136011, and 21500420 for Scientific Research from the Ministry of Education, Culture, Sports, Science, and Technology of Japan (to T.A.), and by NIH grants R01 HL082729 and R01 HL103428 and NSF grant CBET-0933029 (to N.T.).

8. References

- Ashihara, T.; Constantino, J. & Trayanova, N. A. (2008). Tunnel propagation of postshock activations as a unified hypothesis for fibrillation induction and isoelectric window. *Circ Res*, Vol. 102, pp. 737-745
- Chattipakorn, N.; Banville, I.; Gray, R. A. & Ideker, R. E. (2001). Mechanism of ventricular defibrillation for near-defibrillation threshold shocks: a whole-heart optical mapping study in swine. *Circulation*, Vol. 104, pp. 1313-1319
- Chattipakorn, N.; Fotuhi, P. C.; Chattipakorn, S. C. & Ideker, R. E. (2003). Three-dimensional mapping of earliest activation after near-threshold ventricular defibrillation shocks. *J Cardiovasc Electrophysiol*, Vol. 14, pp. 65-69
- Chen, P-S.; Shibata, N.; Dixon, E. G.; Wolf, P. D.; Danieleley, N. D.; Sweeney, M. B.; Smith, W. M. & Ideker, R. E. (1986). Activation during ventricular defibrillation in open-chest dogs: evidence of complete cessation and regeneration of ventricular fibrillation after successful shocks. *J Clin Invest*, Vol. 77, pp. 810-823
- Chen, P-S.; Shibata, N.; Dixon, E. G.; Martin, R. O. & Ideker, R. E. (1986). Comparison of the defibrillation threshold and the upper limit of vulnerability. *Circulation*, Vol. 73, pp. 1022-1028
- Constantino, J.; Long, Y.; Ashihara, T. & Trayanova, N. A. (2010). Tunnel propagation following defibrillation with ICD shocks: hidden postshock activations in the left ventricular wall underlie isoelectric window. *Heart Rhythm*, Vol. 7, pp. 953-961
- Davy, J. M.; Fain, E. S.; Dorian, P. & Winkle, R. A. (1987). The relationship between successful defibrillation and delivered energy in open-chest dogs: reappraisal of the defibrillation threshold concept. *Am Heart J*, Vol. 113, pp. 77-84
- Dosdall, D. J.; Cheng, K. A.; Huang, J.; Allison, J. S.; Allred, J. D.; Smith, W. M. & Ideker, R. E. (2007). Transmural and endocardial Purkinje activation in pigs before local myocardial activation after defibrillation shocks. *Heart Rhythm*, Vol. 4, pp. 758-765
- Entcheva, E.; Trayanova, N. & Claydon, F. J. (1999). Patterns of and mechanisms for shock-induced polarization in the heart: a bidomain analysis. *IEEE Trans Biomed Eng*, Vol. 46, pp. 260-270
- Hwang, G-S.; Hayashi, H.; Tang, L.; Ogawa, M.; Hernandez, H.; Tan, A-Y.; Li, H.; Karagueuzian, H. S.; Weiss, J. N.; Lin, S-F. & Chen, P-S. (2006). Intracellular calcium and vulnerability to fibrillation and defibrillation in Langendorff-perfused rabbit ventricles. *Circulation*, Vol. 114, pp. 2595-2603
- Maisel, W. H. (2006). Pacemaker and ICD generator reliability; meta-analysis of device registries. *JAMA*, Vol. 295, pp. 1929-1934
- Rodriguez, B.; Li, L.; Eason, J. C.; Efimov, I. R. & Trayanova N. A. (2005). Differences between left and right ventricular chamber geometry affect cardiac vulnerability to electric shocks. *Circ Res*, Vol. 97, pp.168-175
- Runsio, M.; Kallner, A.; Kallner, G.; Rosenqvist, M. & Bergfeldt, L. (1997). Myocardial injury after electrical therapy for cardiac arrhythmias assessed by troponin-T release. *Am J Cardiol*, Vol. 79, pp. 1241-1245
- Shibata, N.; Chen, P-S.; Dixon, E. G.; Wolf, P. D.; Danieleley, N. D.; Smith, W. M. & Ideker, R. E. (1988). Influence of shock strength and timing on induction of ventricular arrhythmias in dogs. *Am J Physiol*, Vol. 255, pp. H891-H901

- Shibata, N.; Chen, P-S.; Dixon, E. G.; Wolf, P. D.; Danieleley, N. D.; Smith, W. M. & Ideker, R. E. (1988). Epicardial activation after unsuccessful defibrillation shocks in dogs. *Am J Physiol*, Vol. 255, pp. H902-H909
- Swerdlow, C. D.; Kass, R. M.; O'Connor, M. E. & Chen, P-S. (1998). Effect of shock waveform on relationship between upper limit of vulnerability and defibrillation threshold. *J Cardiovasc Electrophysiol*, Vol. 9, pp. 339-349
- Trayanova, N.; Eason, J. & Aguel, F. (2002). Computer simulations of cardiac defibrillation: a look inside the heart. *Comput Visual Sci*, Vol. 4, pp. 259-270
- Trayanova, N.; Gray, R. A.; Bourn, D. W. & Eason, J. C. (2003). Virtual electrode-induced positive and negative graded responses: new insights into fibrillation induction and defibrillation. *J Cardiovasc Electrophysiol*, Vol. 14, pp. 756-763
- Wang, N-C.; Lee, M-H.; Ohara, T.; Okuyama, Y.; Fishbein, G. A.; Lin, S-F.; Karagueuzian, H. S. & Chen, P-S. (2001). Optical mapping of ventricular defibrillation in isolated swine right ventricles: demonstration of a postshock isoelectric window after near-threshold defibrillation shocks. *Circulation*, Vol. 104, pp. 227-233
- Yashima, M.; Kim, Y-H.; Armin, S.; Wu, T-J.; Miyauchi, Y.; Mandel, W. J., Chen, P-S. & Karagueuzian, H. S. (2003). On the mechanism of the probabilistic nature of ventricular defibrillation threshold. *Am J Physiol Heart Circ Physiol*, Vol. 284, pp. H249-H255

IntechOpen



Cardiac Defibrillation - Mechanisms, Challenges and Implications

Edited by Prof. Natalia Trayanova

ISBN 978-953-307-666-9

Hard cover, 248 pages

Publisher InTech

Published online 26, September, 2011

Published in print edition September, 2011

The only known effective therapy for lethal disturbances in cardiac rhythm is defibrillation, the delivery of a strong electric shock to the heart. This technique constitutes the most important means for prevention of sudden cardiac death. The efficacy of defibrillation has led to an exponential growth in the number of patients receiving implantable devices. The objective of this book is to present contemporary views on the basic mechanisms by which the heart responds to an electric shock, as well as on the challenges and implications of clinical defibrillation. Basic science chapters elucidate questions such as lead configurations and the reasons by which a defibrillation shock fails. Chapters devoted to the challenges in the clinical procedure of defibrillation address issues related to inappropriate and unnecessary shocks, complications associated with the implantation of cardioverter/defibrillator devices, and the application of the therapy in pediatric patients and young adults. The book also examines the implications of defibrillation therapy, such as patient risk stratification, cardiac rehabilitation, and remote monitoring of patient with implantable devices.

How to reference

In order to correctly reference this scholarly work, feel free to copy and paste the following:

Takashi Ashihara, Jason Constantino and Natalia A. Trayanova (2011). Mechanisms of Defibrillation Failure, Cardiac Defibrillation - Mechanisms, Challenges and Implications, Prof. Natalia Trayanova (Ed.), ISBN: 978-953-307-666-9, InTech, Available from: <http://www.intechopen.com/books/cardiac-defibrillation-mechanisms-challenges-and-implications/mechanisms-of-defibrillation-failure>

INTECH
open science | open minds

InTech Europe

University Campus STeP Ri
Slavka Krautzeka 83/A
51000 Rijeka, Croatia
Phone: +385 (51) 770 447
Fax: +385 (51) 686 166
www.intechopen.com

InTech China

Unit 405, Office Block, Hotel Equatorial Shanghai
No.65, Yan An Road (West), Shanghai, 200040, China
中国上海市延安西路65号上海国际贵都大饭店办公楼405单元
Phone: +86-21-62489820
Fax: +86-21-62489821

© 2011 The Author(s). Licensee IntechOpen. This chapter is distributed under the terms of the [Creative Commons Attribution-NonCommercial-ShareAlike-3.0 License](#), which permits use, distribution and reproduction for non-commercial purposes, provided the original is properly cited and derivative works building on this content are distributed under the same license.

IntechOpen

IntechOpen